

## 5.4. Electron-diffraction methods

BY A. W. S. JOHNSON AND A. OLSEN

### 5.4.1. Determination of cell parameters from single-crystal patterns (By A. W. S. Johnson)

#### 5.4.1.1. Introduction

This article treats the recovery of cell axes and angles from (a) a single pattern with suitable Laue zones and (b) two patterns with different zone axes. It is assumed that instrument distortions, if significant, are corrected and that the patterns are free of artefacts such as twinning, double diffraction *etc.* (Edington, 1975). The treatment is valid for convergent-beam, micro and selected-area electron-diffraction patterns and accelerating voltages above approximately 30 kV. Relevant papers are by LePage (1992) and Zuo (1993), and background reading is contained in Edington (1975), Gard (1976), and Hirsch, Howie, Nicholson, Pashley & Whelan (1965).

The basic requirement in the determination of the unit cell of a crystal is to find, from one or more diffraction patterns, the basis vector set,  $\mathbf{a}^*$ ,  $\mathbf{b}^*$ ,  $\mathbf{c}^*$ , of a primitive reciprocal unit cell. The Cartesian components of these vectors form an orientation matrix

$$UB = (\mathbf{a}^*, \mathbf{b}^*, \mathbf{c}^*),$$

which, when inverted, gives the vector components of the corresponding real-space cell. The elements of  $UB$  can be measured directly from the diffraction pattern in millimetres. Define axes  $x$  and  $y$  to be in the recording plane and  $z$  in the beam direction. A point in the diffraction pattern  $x, y, z$  is then related to the indices  $h, k, l$  by

$$\begin{pmatrix} x \\ y \\ z \end{pmatrix} = UB \begin{pmatrix} h \\ k \\ l \end{pmatrix}.$$

Note that points with non-zero  $z$  are observed on the plane  $z = 0$ , see Fig. 5.4.1.1.

The metric  $M$  of  $UB^{-1}$  is used to find the unit-cell edges and angles as

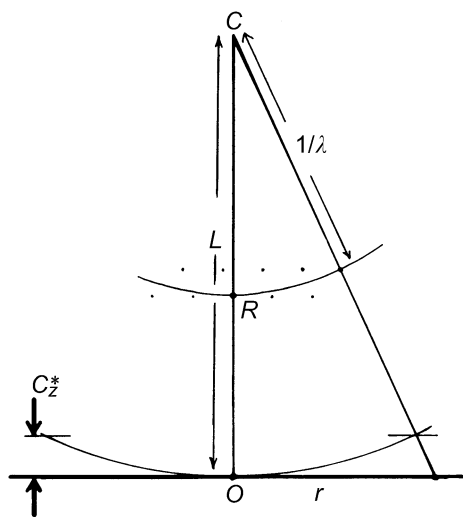


Fig. 5.4.1.1. Diffraction geometry. Crystal at  $C$  with the direct transmitted beam,  $CRO$ , intersecting the reciprocal-lattice origin at  $R$  and the recording plane at normal incidence at  $O$ . The camera length  $L$  is  $CO$  and the reciprocal of the wavelength  $\lambda$  is  $CR$ .

Table 5.4.1.1. Unit-cell information available for photographic recording

	Pattern type	Constants known	Information available
(1)	Zero zone	None or $\lambda$ or $L$	$d$ ratios and interplane angles
(2)		$L\lambda$ or $L$ and $\lambda$	$d$ values and interplane angles
(3)	Multiple zone	None or $L$	As for (1)
(4)		$L\lambda$	As for (2)
(5)		$\lambda$	Unit-cell axial ratios and angles
(6)		$L$ and $\lambda$	Unit-cell axes and angles
(7)	Two or more zero-zone patterns*	None or $L$	As for (5)
(8)		$L\lambda$	As for (6)

\* See text, Subsection 5.4.1.2.

$$M = UB^{-1} \cdot (UB^{-1})^T,$$

where  $T$  means the transpose. Then,

$$M = \begin{pmatrix} \mathbf{a} \cdot \mathbf{a} & \mathbf{a} \cdot \mathbf{b} & \mathbf{a} \cdot \mathbf{c} \\ \mathbf{a} \cdot \mathbf{b} & \mathbf{b} \cdot \mathbf{b} & \mathbf{b} \cdot \mathbf{c} \\ \mathbf{a} \cdot \mathbf{c} & \mathbf{b} \cdot \mathbf{c} & \mathbf{c} \cdot \mathbf{c} \end{pmatrix}$$

gives

$$a = L\lambda(\mathbf{a} \cdot \mathbf{a})^{1/2},$$

$$b = L\lambda(\mathbf{b} \cdot \mathbf{b})^{1/2},$$

$$c = L\lambda(\mathbf{c} \cdot \mathbf{c})^{1/2},$$

$$\cos \gamma = \mathbf{a} \cdot \mathbf{b} / (\mathbf{a} \cdot \mathbf{a} \mathbf{b} \cdot \mathbf{b})^{1/2},$$

$$\cos \beta = \mathbf{a} \cdot \mathbf{c} / (\mathbf{a} \cdot \mathbf{a} \mathbf{c} \cdot \mathbf{c})^{1/2},$$

and

$$\cos \alpha = \mathbf{b} \cdot \mathbf{c} / (\mathbf{b} \cdot \mathbf{b} \mathbf{c} \cdot \mathbf{c})^{1/2},$$

where  $L$  is the effective distance between the diffracting crystal and the recording plane and  $\lambda$  is the wavelength. These quantities are defined in Fig. 5.4.1.1 together with the nomenclature and geometrical relationships required in this article.

If necessary, the cell is reduced to the Bravais cell according to the procedures given in *IT A* (1983, Chapter 9.3), before calculating the metric.

In practice, there may be a difficulty in choosing a vector set that describes a *primitive* reciprocal cell. Although a record of any reasonably dense plane of reciprocal space immediately exposes two basis vectors of a cell, the third vector lies out of the plane of the diffraction pattern containing the first two vectors and may not be directly measurable. Hence, some care must be taken to ensure that the third vector chosen makes the cell

## 5. DETERMINATION OF LATTICE PARAMETERS

primitive. This presents no difficulty in the non-zero-zone analysis given in Subsection 5.4.1.3 but needs consideration when two patterns are used as described in Subsection 5.4.1.2.

Unit-cell parameters may be partly or fully determined depending on the extent of knowledge of the effective camera length  $L$  and wavelength  $\lambda$ , and upon the type and number of patterns. The different situations are distinguished in Table 5.4.1.1 for photographic recording. Note that  $L$  is simply a magnification factor.

The accuracy of the non-zero-zone analysis described in Subsection 5.4.1.3 will depend on the influence of spiral, radial, and elliptical distortions. The camera length and wavelength need to be known to better than 1%.

For measurements made using microscope deflector systems, a knowledge of  $L$  may not be required depending on the location of the deflectors in the microscope column. Instead, the calibration factor of the deflectors, in suitable units, will replace  $L$ .

### 5.4.1.2. Zero-zone analysis

Two patterns are required that represent different sections through the reciprocal lattice. The angle of rotation  $p$  between these sections must be known, as well as the trace of the rotation axis in the plane of the pattern. Define the plane of the first pattern as the  $xy$  plane with the  $x$  axis, for convenience, coincident with the trace of the rotation axis. The coordinates  $x_0, y_0$  of reflections in the first pattern are then measured. The coordinates  $x_1, y_1$  of spots in the patterns rotated by  $p$  relative to the first pattern are then measured, care being taken to align the trace of the rotation axis with the  $x$  axis of the measuring equipment for each pattern. The coordinates of these reflections are then reduced to the coordinate system of the first pattern by the relations  $x_0 = x_1, y_0 = y_1 \cos(p), z_0 = y_1 \sin(p)$ . The coordinates of all reflections measured are placed in a table that is scanned to extract the three shortest non-coplanar vectors. If the patterns come from dense, neighbouring zones, it is likely that these vectors define a primitive cell.

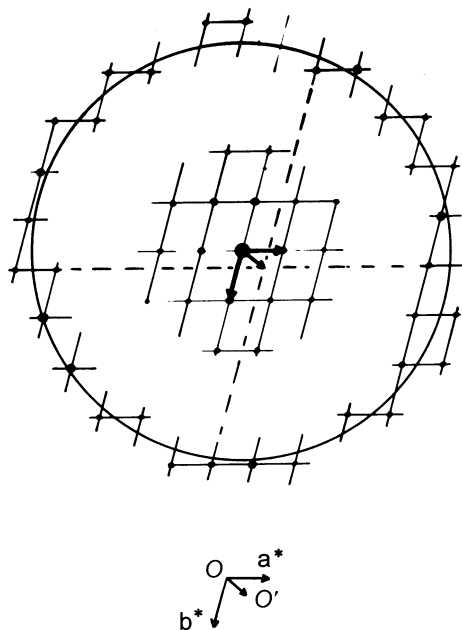


Fig. 5.4.1.2. A diffraction pattern with the crystal oriented at a zone axis. The lower diagram shows the zero-zone vectors  $\mathbf{a}^*$  and  $\mathbf{b}^*$ , and  $OO'$ , the projection on the  $xy$  plane of  $\mathbf{c}^*$ .

### 5.4.1.3. Non-zero-zone analysis

One pattern with well defined Laue zones taken at an arbitrary zone allows the recovery of a third vector not in the plane of the pattern. First find the components for the two shortest zero-zone vectors  $\mathbf{a}^*$  and  $\mathbf{b}^*$  (see Fig. 5.4.1.2). For the third vector, measure the  $x$  and  $y$  coordinates of a non-zero-zone vector. These are then transformed to components in the coordinate system defined by the two shortest vectors of the zero zone. Then the fractional part of each transformed component is taken. If the vector comes from a Laue zone of order  $n$ , these fractional parts must be divided by  $n$ . A transformation back to Cartesian coordinates gives the  $x$  and  $y$  components of the third vector  $\mathbf{c}^*$ , point  $O'$  in Fig. 5.4.1.2. In practice, it is best to measure a set of vectors at roughly equal angles around the zone so that an average can be taken to improve accuracy.

For certain space groups and special orientations, it is possible for half of the zero-zone reflections to be absent. If sufficient non-zero-zone vectors have been measured, two different vectors  $OO'$  should be found. New axes  $(\mathbf{a}^* + \mathbf{b}^*)/2$  and  $(\mathbf{a}^* - \mathbf{b}^*)/2$  must then be chosen and the  $x$  and  $y$  coordinates of  $\mathbf{c}^*$  recalculated.

The  $z$  component of  $\mathbf{c}^*$  is obtained (Fig. 5.4.1.1) from

$$c_z^* = L[1 - 1/(1 + r^2/L^2)^{1/2}]/n,$$

where  $r$  is the radius of the Laue circle of order  $n$ .

We now have the orientation matrix  $\mathbf{UB}$  as

$$\mathbf{UB} = \begin{pmatrix} a_x^* & b_x^* & c_x^* \\ a_y^* & b_y^* & c_y^* \\ 0 & 0 & c_z^* \end{pmatrix},$$

and the measurement of the pattern is complete.

After transformation of the axes defined by  $\mathbf{UB}$  to the Bravais axes, the inverse of the resulting  $\mathbf{UB}_{\text{Bravais}}$  will index the pattern using

$$\begin{pmatrix} h \\ k \\ l \end{pmatrix} = \mathbf{UB}_{\text{Bravais}}^{-1} \begin{pmatrix} x \\ y \\ z \end{pmatrix}.$$

### 5.4.2. Kikuchi and HOLZ techniques (By A. Olsen)

Lattice-parameter determination based on selected-area electron-diffraction patterns requires accurate calibration of the camera constant  $K$ . This constant depends on the electron wavelength  $\lambda$  and the camera length  $L$  and is given by  $K = \lambda L$ . Because the camera constant cannot be determined with sufficient accuracy in a transmission electron microscope, a number of methods for determination of lattice parameters (or electron wavelength)

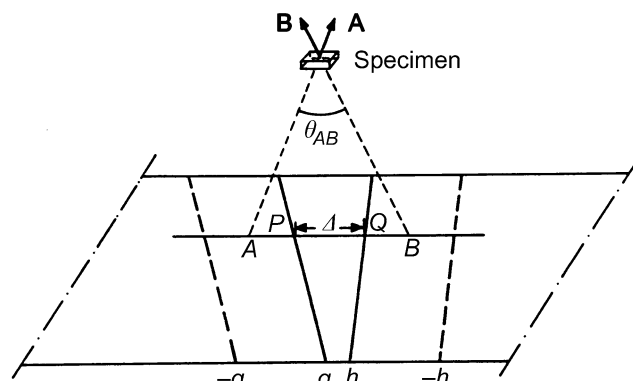


Fig. 5.4.2.1. Schematic diagram showing the geometry of a Kikuchi pattern.

#### 5.4. ELECTRON-DIFFRACTION METHODS

have been developed based on Kikuchi or HOLZ (high-order Laue zone) lines (Uyeda, Nonoyama & Kogiso, 1965; Høier, 1969; Olsen, 1976a; Jones, Rackham & Steeds, 1977). In these methods, the lattice parameters can be determined, provided the electron wavelength is known (or *vice versa*) without knowing the value of  $K$ .

In the method of Uyeda *et al.* (1965), the electron wavelength can be determined from a single Kikuchi pattern provided that the lattice parameters of the crystal are known. Fig. 5.4.2.1 illustrates the geometry involved in the method. **A** and **B** are two zone axes of the specimen. The pairs of Kikuchi lines  $g$ ,  $-g$  and  $h$ ,  $-h$  belong to the zones **A** and **B**, respectively. The points  $P$  and  $Q$  are the intersections of the Kikuchi lines  $g$  and  $h$  with the line  $AB$ .

As a first approximation, the wavelength of the electrons is given by

$$\lambda = \theta_{AB}/[(1/2d_P) + (1/2d_Q) + (\Delta/D)(1/d)], \quad (5.4.2.1)$$

where  $D$  is the measured distance between the two Kikuchi lines in either of the pairs and  $d$  is the corresponding interplanar spacing.  $\theta_{AB}$  is the angle between the zone axes **A** and **B**. When the Kikuchi pattern is indexed,  $\theta_{AB}$  and  $d$  can be calculated from the known lattice parameters of the specimen.  $d_P$  and  $d_Q$  are effective interplanar spacings and are given by

$$\begin{aligned} d_P &= d_g \sin \varphi_g, \\ d_Q &= d_h \sin \varphi_h; \end{aligned} \quad (5.4.2.2)$$

$d_g$  and  $d_h$  are the interplanar spacings corresponding to  $g$  and  $h$ , respectively. The angle  $\varphi_g$  (or  $\varphi_h$ ) is the angle between the lattice plane  $g$  (or  $h$ ) and the plane defined by **A** and **B**. These angles are given by

$$\begin{aligned} \sin \varphi_g &= \mathbf{g} \times (\mathbf{A} \times \mathbf{B}) / (|\mathbf{g}| \cdot |\mathbf{A} \times \mathbf{B}|), \\ \sin \varphi_h &= \mathbf{h} \times (\mathbf{A} \times \mathbf{B}) / (|\mathbf{h}| \cdot |\mathbf{A} \times \mathbf{B}|). \end{aligned} \quad (5.4.2.3)$$

The values of  $d_P$  and  $d_Q$  to be used in (5.4.2.1) can be calculated from (5.4.2.2) and (5.4.2.3).

If  $\Delta$  and  $D$  are measured on the photographic plate or a print of any magnification, the electron wavelength can be calculated by using (5.4.2.1). Only the ratio  $(\Delta/D)$  is required for the determination of  $\lambda$ . The distance  $AB$  is not required. The points  $A$  and  $B$  are used only to fix the points  $P$  and  $Q$ .  $A$  and  $B$  do not need to fall inside the photographic plate when a Kikuchi pattern is symmetrical across the line  $AB$ , because in such cases  $P$  and  $Q$  can be determined from intersections of Kikuchi lines that are symmetrical with each other. The expression for  $\lambda$  in (5.4.2.1) is only a first approximation. More accurate expressions can be found in the paper by Uyeda *et al.* (1965).

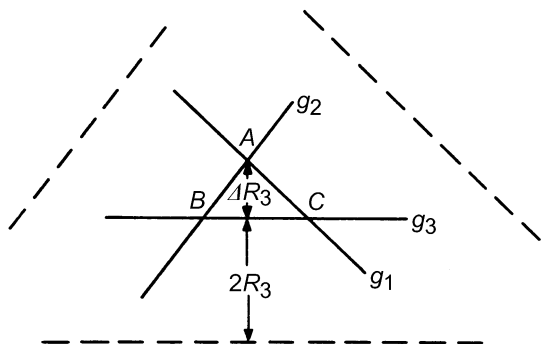


Fig. 5.4.2.2. Schematic diagram of three Kikuchi lines that nearly intersect at the same point.

A simpler and more accurate method has been developed by Høier (1969). He showed that in the cubic case it is possible to determine the ratio between the lattice parameter  $a$  and the electron wavelength  $\lambda$  with a relative accuracy of 0.1%. Only two quantities have to be measured on the photographic plate or a print at any magnification: the height of a triangle formed by three Kikuchi lines and one separation between a defect-excess line pair (Fig. 5.4.2.2). If three indexed Kikuchi lines  $g_i$  intersect at the same point on a photographic plate, the following equations can be derived from Bragg's law:

$$2\mathbf{g}_i \mathbf{K} = -|\mathbf{g}_i|^2, \quad i = 1, 2, 3. \quad (5.4.2.4)$$

In addition, the length of  $\mathbf{K}$  is equal to the electron wavelength

$$|\mathbf{K}| = 1/\lambda_i, \quad (5.4.2.5)$$

where the wavelength is written  $\lambda_i$  for generality (for electrons,  $\lambda_i = \lambda$ ). If the Kikuchi lines  $g_i$  do not belong to the same zone, (5.4.2.4) and (5.4.2.5) can be solved and  $a/\lambda$  determined.

Exact triple intersections are rare. A practical method as proposed by Høier (1969) is therefore based on three lines that nearly intersect at the same point (Fig. 5.4.2.2). The dimensions of the triangle  $ABC$  in Fig. 5.4.2.2 change with  $\lambda$ . Let us assume that only the wavelength in the beam giving the  $g_3$  reflection varies. The increment  $\Delta\lambda_3$  necessary to shift the line  $g_3$  to  $A$  is then determined by

$$\lambda_3 = \lambda + \Delta\lambda_3 \sim \lambda(1 + \Delta R_3/R_3). \quad (5.4.2.6)$$

By measuring the height in the triangle  $ABC$  and the line separation  $2R_3$ , the wavelength to be used in (5.4.2.5) can be calculated and the ratio  $a/\lambda$  determined. Care must be taken to avoid areas where the lines are displaced from kinematical positions owing to dynamical interactions.

The method of Høier (1969) for cubic crystals was later extended to lower-symmetry cases (triclinic) by Olsen (1976a), who also developed computer programs for least-squares refinement of the lattice parameters. The derivation of the equations for the procedure is carried out in the following in a way slightly different from that described by Olsen (1976a).

If three Kikuchi lines  $\mathbf{g}_i(h_i, k_i, l_i)$  not belonging to the same zone intersect at the same point on the photographic plate, the direction  $\mathbf{K}$  from the origin of the Ewald sphere to the intersection point of the Kikuchi lines is given by Bragg's law:

$$2\mathbf{g}_i \mathbf{K} = -|\mathbf{g}_i|^2, \quad i = 1, 2, 3. \quad (5.4.2.7)$$

The length of the vector  $\mathbf{K}$  is given by

$$|\mathbf{K}| = 1/\lambda, \quad (5.4.2.8)$$

where  $\lambda$  is the electron wavelength.

Because triple intersections are rare, a practical method is therefore based on three lines that nearly intersect at the same point, as proposed by Høier (1969). In order to obtain an exact intersection, one of the lines can be changed from  $\mathbf{g}_i$  to  $\mathbf{g}_i + \Delta\mathbf{g}_i$ , where  $\Delta\mathbf{g}_i$  is a vector approximately parallel to  $\mathbf{g}_i$ . For this Kikuchi line (in the following assumed to be line no. 3), the Bragg condition (5.4.2.7) gives

$$2(\mathbf{g}_3 + \Delta\mathbf{g}_3) \mathbf{K} = -(\mathbf{g}_3 + \Delta\mathbf{g}_3)^2. \quad (5.4.2.9)$$

For a pair of Kikuchi lines, the simple relation

$$2\Delta\mathbf{g}_3 = (\Delta R_3/R_3)\mathbf{g}_3 \quad (5.4.2.10)$$

holds, where  $2R_3$  is the line separation measured on the photographic plate of the centres of the two Kikuchi lines.  $\Delta R_3$  is the shift (measured on the plate) in the position of one of the lines in order to obtain an exact triple intersection.

## 5. DETERMINATION OF LATTICE PARAMETERS

Substitution of (5.4.2.10) into (5.4.2.9) gives

$$2\mathbf{g}_3\mathbf{K} = -|\mathbf{g}_3|^2(1 + \Delta R_3/R_3). \quad (5.4.2.11)$$

From  $n$  measurements of intersections, the following equations are obtained:

$$h_{ji}u_j + k_{ji}v_j + l_{ji}w_j = -(1/2)(1/d_{ji})^2(1 + \delta_{i3}\Delta R_{j3}/R_{j3}),$$

$$i = 1, 2, 3, \quad j = 1, 2, \dots, n, \quad (5.4.2.12)$$

where  $h_{ji}, k_{ji}, l_{ji}$  are the indices (given in reciprocal space) of the Kikuchi lines,  $\delta_{i3}$  is the Kronecker delta,  $u_j, v_j, w_j$  are the indices (given in real space) of the direction  $\mathbf{K}_j$  to the intersection number  $j$ , and  $d_{ji}$  is the interplanar spacing corresponding to the reflection  $h_{ji}, k_{ji}, l_{ji}$  and can be expressed in terms of the cell dimensions in real space. The length of the  $\mathbf{K}_j$  vectors can also be expressed in terms of the lattice parameters in real space  $a, b, c, \alpha, \beta$ , and  $\gamma$  as

$$|\mathbf{K}_j| = (u_j^2a^2 + v_j^2b^2 + w_j^2c^2 + 2u_jv_jab\cos\alpha + 2u_jw_jac\cos\beta + 2v_jw_jbc\cos\gamma)^{1/2}. \quad (5.4.2.13)$$

Equations (5.4.2.12) can be solved with respect to  $u_j, v_j, w_j$ , and  $\mathbf{K}_j$  can then be expressed in terms of the lattice parameters by substituting the expressions for  $u_j, v_j, w_j$  from (5.4.2.12) into (5.4.2.13).

If the number of intersections is greater than the number of unknown lattice parameters, a least-squares-refinement procedure can be used. This involves minimizing the function

$$Q = \sum_j (|\mathbf{K}_j| - 1/\lambda)^2. \quad (5.4.2.14)$$

Because the expression for  $Q$  is non-linear in the lattice parameters, a refinement procedure can be used to solve the equations derived from (5.4.2.14) using the least-squares procedure. The accuracy in the lattice parameters or wavelength can be found by statistical methods. A computer program for refinement of the lattice parameters (or electron wavelength) is available (Olsen, 1976b). In this program, some of the lattice parameters can be held constant or kept equal during the refinement.

Methods based on measurements of distances between zone axes (poles) in the Kikuchi patterns (Thomas, 1970) are not very accurate because optical distortions make long-distance measurements inaccurate on the photographic plate or a magnified print.

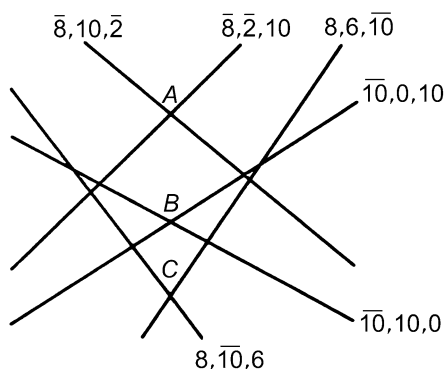


Fig. 5.4.2.3. Schematic diagram showing the indexing of the most prominent lines in the selected-area channelling pattern near the [111] zone of Si. Accelerating voltage: 25 kV.

The methods by Høier (1969) and Olsen (1976a) are based on 'near intersections'. Better accuracy may be obtained if the high voltage can be varied in order to obtain exact intersections. A simple method for determination of lattice parameters can be applied for crystals with symmetry as low as orthorhombic (Gjønnes & Olsen, 1984). The method is a simplified version of the Uyeda *et al.* (1965) method. If two parallel Kikuchi lines belonging to different zones overlap, then:

$$2\mathbf{g}_i\mathbf{K} = -|\mathbf{g}_i|^2, \quad i = 1, 2;$$

$$(\mathbf{g}_1 \times \mathbf{g}_2)\mathbf{K} = 0, \quad |\mathbf{K}| = 1/\lambda. \quad (5.4.2.15)$$

These equations can be solved to give the ratio between lattice parameter and electron wavelength.

A simple, rapid procedure for accelerating-voltage (or electron-wavelength) determination of a transmission electron microscope has been described by FitzGerald & Johnson (1984). In their method, it is necessary to measure the ratio of two easily found distances between points defined by the intersections of Kikuchi lines near the {111} zone of a silicon crystal. It is not necessary to index the Kikuchi lines, because the method is based on (a) a particular crystal and (b) an easily recognizable crystal orientation, and because the points between which distances need to be measured are specified in their paper and can be easily found. Polynomials for converting the distance measurements both to electron wavelength and to accelerating voltage are given for the range from 100 to 200 kV. A 300 K temperature change must occur (temperature coefficient of  $3 \times 10^{-6}$  K) before the error in the lattice parameter of silicon due to thermal expansion becomes significant.

A method for measuring small local changes in the lattice parameter of bulk specimens based on selected-area channelling patterns has been described by Walker & Booker (1982). The method utilizes the small changes in the position of high-index channelling lines due to small changes in the lattice parameters, and is based on scanning electron microscopy (SEM). The method is rapid and convenient, is suitable for bulk specimens, and can be applied to areas only a few micrometres across. The method has been used for Si and GaP and is in this case based on the intersection of pairs of  $\bar{8},10,2$ ,  $\bar{10},10,0$ ,  $8,\bar{10},6$  type lines (the points A, B, and C in Fig. 5.4.2.3). Selected-area channelling patterns from Si and GaP obtained under precisely the same conditions have the same characteristic array of lines, but with slightly different distances AB and BC. The detection limit of this method is at present 3 parts in  $10^4$ .

When a small electron probe is used to illuminate a crystal, as in convergent-beam electron diffraction (CBED), very fine lines are often found in the diffraction discs (Steeds, 1979). These lines are called HOLZ lines. They are due to upper-layer diffraction effects and can be used in lattice-parameter determination (Rackham, Jones & Steeds, 1974; Jones, Rackham & Steeds, 1977). For highest accuracy, relatively thick crystals are required. The limitation to the accuracy is set either by the weakness of the lines or by energy losses in the specimen. Relative changes in the lattice parameters can be measured to an accuracy of 1 part in  $10^4$ , whereas the accuracy in the absolute determination of lattice parameters is typically of an order of magnitude worse. The lattice parameters can be measured from crystal regions as small as 20 nm in diameter with an accuracy better than 1 part in  $10^3$ . If more accurate results are desired, it is necessary to make measurements on lines that are not affected by interactions between HOLZ reflections.

## REFERENCES

## 5.3 (cont.)

- Windisch, D. & Becker, P. (1990). *Silicon lattice parameters as an absolute scale of length for high precision measurements of fundamental constants*. *Phys. Status Solidi A*, **118**, 379–388.
- Wołczyrz, M. & Lukaszewicz, K. (1982). *The evaluation of crystal perfection by means of the asymmetric Bragg reflections*. *J. Appl. Cryst.* **15**, 406–411.
- Wołczyrz, M., Pietraszko, A. & Lukaszewicz, K. (1980). *The application of asymmetric Bragg reflections in the Bond method of measuring lattice parameters*. *J. Appl. Cryst.* **13**, 12–16.
- Wölfel, E. R. (1971). *A new film instrument for the exploration of reciprocal space*. *J. Appl. Cryst.* **4**, 297–302.
- Woolfson, M. M. (1970). *An introduction to X-ray crystallography*. Cambridge University Press.
- Yakowitz, H. (1966a). *Effect of sample thickness and operating voltage on the contrast of Kossel transmission photographs*. *J. Appl. Phys.* **37**, 4455–4458.
- Yakowitz, H. (1966b). *Precision of cubic lattice parameter measurement by the Kossel technique*. *The electron microprobe*, edited by T. D. McKinley, K. F. J. Heinrich & D. B. Wittry, pp. 417–438. New York: John Wiley.
- Yakowitz, H. (1969). *The divergent beam X-ray technique*. *Advances in electronics and electron physics*, edited by A. J. Tousimis & L. Marton, Suppl. 6, pp. 361–431. New York: Academic Press.
- Yakowitz, H. (1972). *Use of divergent-beam X-ray diffraction to measure lattice expansion in LiF as a function of thermal-neutron dose up to  $6 \times 10^{16}$  nvt*. *J. Appl. Phys.* **43**, 4793–4794.
- Zolotoyabko, E., Sander, B., Komem, Y. & Kantor, B. (1993). *Improved strain analysis in semiconductor crystals by X-ray diffractometry enhanced with ultrasound*. *Appl. Phys. Lett.* **63**, 1540–1542.

## 5.4.1

- Edington, J. W. (1975). *Electron diffraction in the electron microscope*. *Monographs in practical electron microscopy in materials science*, No. 2. Eindhoven: N. V. Philips Gloeilampenfabrieken.
- Gard, J. A. (1976). *Electron microscopy in mineralogy*, p. 52. Berlin: Springer.
- Hirsch, P. B., Howie, A., Nicholson, R. B., Pashley, D. W. & Whelan, M. J. (1965). *Electron microscopy of thin crystals*. London: Butterworth.
- International Tables for Crystallography* (1983). Vol. A. Dordrecht: Kluwer Academic Publishers.
- LePage, Y. (1992). *Ab initio primitive cell parameters from single convergent beam patterns: a converse route to the identification of microcrystals with electrons*. *Miscrosc. Res. Tech.* **21**, 158–165.

- Zuo, J. M. (1993). *New method of Bravais lattice determination*. *Ultramicroscopy*, **52**, 459–464.

## 5.4.2

- FitzGerald, J. D. & Johnson, A. W. S. (1984). *A simplified method of electron microscope voltage measurement*. *Ultramicroscopy*, **12**, 231–236.
- Gjønnnes, J. & Olsen, A. (1984). *Analytical electron microscopy*. *JEOL News*, **22E**, 13–18.
- Høier, R. (1969). *A method to determine the ratio between lattice parameter and electron wavelength from Kikuchi line intersections*. *Acta Cryst.* **A25**, 516–518.
- Jones, P. M., Rackham, G. M. & Steeds, J. W. (1977). *Higher order Laue zone effects in electron diffraction and their use in lattice parameter determination*. *Proc. R. Soc. London Ser. A*, **354**, 197–222.
- Olsen, A. (1976a). *Lattice parameter determination using Kikuchi-line intersections: application to olivine and feldspar*. *J. Appl. Cryst.* **9**, 9–13.
- Olsen, A. (1976b). *Determination of lattice constants using Kikuchi line intersections*. Solid State Group Report Series. Institute of Physics, University of Oslo, Norway.
- Rackham, G. M., Jones, P. M. & Steeds, J. W. (1974). *Upper layer diffraction effects in zone axis patterns*. Proceedings of the Eighth International Congress on Electron Microscopy, Canberra, Australia, pp. 336–337.
- Steeds, J. W. (1979). *Convergent beam electron diffraction*. *Introduction to analytical electron microscopy*, edited by J. J. Hren, J. I. Goldstein & D. C. Joy, pp. 387–422. New York: Plenum.
- Thomas, G. (1970). *Kikuchi electron diffraction and applications*. *Modern diffraction and imaging techniques in material science*, edited by S. Amelinckx, S. Gevers, G. Remaut & J. Van Landuyt, pp. 131–185. Amsterdam: North-Holland.
- Uyeda, R., Nonoyama, M. & Kogiso, M. (1965). *Determination of the wavelength of electrons from a Kikuchi pattern*. *J. Electron Microsc.* **14**, 296–300.
- Walker, A. R. & Booker, G. R. (1982). *A selected-area channelling pattern (SACP) method for measuring small local changes in lattice parameter with bulk specimens*. *Electron microscopy 1982*, Vol. 1, pp. 651–652. Hamburg: Elsevier.

## 5.5

- Fischer, P., Zolliker, P., Meier, B. H., Ernst, R. R., Hewat, A. W., Jorgensen, J. D. & Rotella, F. J. (1986). *Structure and dynamics of terephthalic acid from 2 to 300 K*. *J. Solid State Chem.* **61**, 109–125.